Inorganic Chemistry
Article
Cite This: Inorg. Chem. 2019, 58, 6832−6844
pubs.acs.org/IC

Magnesium(II) D-Gluconate Complexes Relevant to Radioactive Waste Disposals: Metal-Ion-Induced Ligand Deprotonation or Ligand-Promoted Metal-Ion Hydrolysis?

Bence Kutus,*[,†,‡] Csilla Dudás,[‡] Eszter Orbán,[‡] Alexandru Lupan,[§] Amr A. A. Attia,[§] István Pálinkó,[‡] Pál Sipos,[‡] and Gábor Peintler[‡]

[†]Department of Molecular Spectroscopy, Max Planck Institute for Polymer Research, D-55128 Mainz, Germany
[‡]Institute of Chemistry, University of Szeged, H-6720 Szeged, Hungary
[§]Department of Chemistry, Babeş-Bolyai University, RO-400028 Cluj-Napoca, Romania

Supporting Information

ABSTRACT: The complexation equilibria between Mg^{2+} and D-gluconate ($Gluc^-$) ions are of particular importance in modeling the chemical speciation in low- and intermediate-level radioactive waste repositories. NMR measurements and potentiometric titrations conducted at 25 °C and 4 M ionic strength revealed the formation of the $MgGluc^+$, $MgGlucOH^0$, $MgGluc(OH)_2^-$, and $Mg_3Gluc_2(OH)_4^0$ complexes. The trinuclear species provides indirect evidence for the existence of multinuclear magnesium(II) hydroxido complexes, whose formation was proposed earlier but has not been confirmed yet. Additionally, speciation calculations demonstrated that $MgCl_2$ can markedly decrease the solubility of thorium(IV) at low ligand concentrations. Regarding the structure of $MgGluc^+$, both IR spectra and density functional theory (DFT) calculations indicate the monodentate coordination of $Gluc^-$. By the potentiometric data, the acidity of the water molecules is higher in the $MgGluc^+$ and $MgGlucOH^0$ species than in the $Mg(H_2O)_6^{2+}$ aqua ion. On the basis of DFT calculations, this ligand-promoted hydrolysis is caused by strong hydrogen bonds forming between $Gluc^-$ and $Mg(H_2O)_6^{2+}$. Conversely, metal-ion-induced ligand deprotonation takes place in the case of calcium(II) complexes, giving rise to salient variations on the NMR spectra in a strongly alkaline medium.

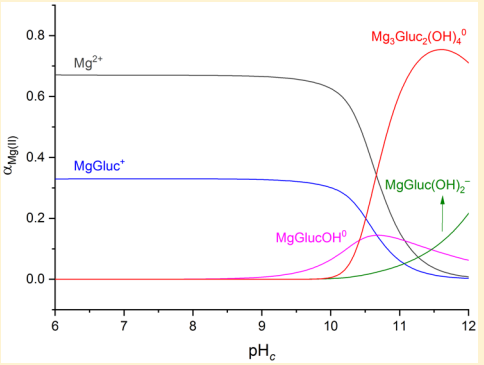

INTRODUCTION

The chemical behavior of actinides in aqueous solutions is of general importance for the disposal of nuclear waste in underground salt mines. The solubility of actinide hydroxides in the so-called pore water is determined by various factors, such as the pH, ionic strength, presence of complexing agents, etc. Portland cement, used for the formulation of cementitious materials,[1] has a large impact on the solution pH. The pH of the pore water is known to increase from neutral to ca. 12.5 because of the dissolution of $Ca(OH)_2(s)$.[2] In underground salt mines, concentrated $MgCl_2$- or NaCl-containing salt brines are supposed to form as a result of the incidental intrusion of water.[3] Bube and co-workers reported that, for brines containing ≈3.8 M $MgCl_2$, the pH increases to ≈12, while most of the Mg^{2+} ions are replaced by Ca^{2+} ions.[3] In leachant solutions containing ≈5.4 M NaCl, the pH becomes as high as 13.

In principle, a highly caustic medium leads to the precipitation of radionuclides, thereby lowers their mobility as well as their release to the geosphere. The presence of various organic molecules, however, may result in an increase of the solubility through the formation of stable metal complexes. D-Gluconate ($Gluc^-$; Scheme 1), being used as an additive in cement,[4] is likely to be present in underground repositories; thus, it is regarded as a general model compound for organic contaminants. $Gluc^-$ is known to chelate thorium(IV),[5,6] uranium(IV),[7] uranium(VI),[8,9] neptunium(IV),[10] plutonium(IV),[11,12] and americium(III)[13] in an alkaline medium.

Scheme 1. Structural Formula of $Gluc^-$

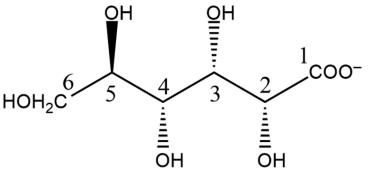

In a caustic medium, one of the OH groups of $Gluc^-$ undergoes deprotonation:

$$Gluc^- = GlucH_{-1}^{2-} + H^+ \quad (1)$$

Received: January 30, 2019
Published: May 8, 2019

DOI: 10.1021/acs.inorgchem.9b00289
Inorg. Chem. 2019, 58, 6832−6844

The corresponding concentration stability constant, K_a, reads as

$$K = \frac{[\mathrm{GlucH}_{-1}^{2-}][\mathrm{H}^+]}{[\mathrm{Gluc}^-]c^\circ} \quad (2)$$

where c° is the standard molar concentration, 1 mol·dm^{-3}. In concentrated electrolyte solutions, the pK was found to be 13.7 (I = 1 M)[14,15] and 14.1 (I = 4 M).[16] Additionally, the deprotonation reaction was invoked to explain the solubility curve of $UO_2(OH)_2(s)$[9] as well as $Th(OH)_4(s)$[5,17] in the presence of $Gluc^-$. The pK of the $ThGluc(OH)_4^-$ aqueous species was calculated to be 9.2 (at infinite dilution).[17] In conclusion, deprotonation of $Gluc^-$ occurs more readily in its metal-bound form compared to the free ligand.

The solubility of actinides can be affected by $CaCl_2$ and/or $MgCl_2$; both salts are expected to be present at high concentrations.[3] First, stable binary complexes forming between Ca^{2+} or Mg^{2+} and $Gluc^-$ ions may suppress the formation of actinide gluconate species, resulting in a decrease of the solubility. For calcium(II), the formation of $CaGlucOH^0$ was detected above pH ≈ 11, while the multinuclear $Ca_2Gluc(OH)_3^0$ and $Ca_3Gluc_2(OH)_4^0$ complexes are the predominant ones at higher $CaCl_2$ and ligand concentrations.[15]

Second, the formation of ternary species consisting of calcium(II), actinide(IV), and gluconate ions increases the solubility. For thorium(IV), the $CaThGluc_2(OH)_4^0$ complex was proposed to elucidate the sorption properties of thorium(IV) onto calcite at pH = 13.3.[13] The formation of this ternary species can be promoted via the mononuclear $CaGlucOH^0$:

$$Th(OH)_4(s) + 2CaGlucOH^0 = CaThGluc_2(OH)_4^0 + Ca^{2+} + 2OH^- \quad (3)$$

Ternary complexes with similar stoichiometry and stability might be formed with Mg^{2+} ions as well. Contrary to Ca^{2+}/$Gluc^-$ complexes, the literature concerning Mg^{2+}/$Gluc^-$ interactions is sporadic. In an early paper, the $MgGluc^+$ species was reported to form at neutral pH.[18] Using IR and ^{1}H NMR spectroscopic means at 25 °C, it was found that the interaction with Mg^{2+} mainly localizes to the carboxylate group of $Gluc^-$.[19] Above ≈35 °C, ^{13}C NMR relaxation studies indicated the additional participation of the terminal hydroxymethyl group (C6-OH; Scheme 1).[20] Alteration of the coordination mode was interpreted in terms of conformational changes: at T < 30 °C, $Gluc^-$ exists in solution as a mixture of the planar (zigzag) and bent-chain forms. With increasing temperature, however, the bent-chain conformer becomes predominant,[20−23] rendering the simultaneous coordination of COO^- and C6-OH possible.

In contrast to Ca^{2+}, the complexation equilibria between Mg^{2+} and $Gluc^-$ ions in the alkaline pH regime were not studied. The formation of such coordination compounds may have a marked influence on the solubility of actinides in the presence of $Gluc^-$. Thus, for modeling the solubility and aqueous speciation of these metal ions in $MgCl_2$-containing solutions, a quantitative description of the Mg^{2+}/$Gluc^-$/OH^- system is indispensable. Furthermore, to reveal the binding sites of the ligand and to make reliable comparisons with the calcium(II) complexes, structural analysis of the magnesium(II) species is necessary.

In this Article, we report on the solution equilibria of magnesium(II) gluconate complexes forming in a neutral-to-alkaline medium. The complexation reactions were studied by potentiometry, IR as well as ^{1}H and ^{13}C NMR spectroscopies. Additionally, the experiments were augmented with quantum-chemical computations. The results are discussed with respect to (1) the effect of $MgCl_2$ on the solubility of thorium(IV) and (2) the possible structures of the magnesium(II) gluconate complexes in comparison with the calcium(II) ones.

EXPERIMENTAL SECTION

Reagents and Solutions. NaGluc (≥98%, Acros Organics), $MgCl_2·6H_2O$ (ACS grade, VWR Chemicals), $CaCl_2·2H_2O$ (ACS grade, VWR Chemicals), and NaCl (analytical reagent grade, VWR Chemicals) were used without further purification. Stock solutions of NaGluc, $MgCl_2$, and $CaCl_2$ were prepared by dissolving the salts in Milli-Q Millipore water. The exact concentration of the Mg^{2+} or Ca^{2+} ions was determined by ethylenediaminetetraacetic acid titration.

A 1 M stock solution of NaOH was prepared by diluting a carbonate-free 50% (w/w) NaOH prepared by the procedure reported in ref 24. The NaOH solution was then standardized against HCl. The 1 M stock solution of HCl was made by volumetric dilution of ≈37% (w/w) HCl (analytical reagent grade, VWR Chemicals), and its concentration was determined via titration of a $KHCO_3$ solution.

Potentiometric Titrations. The potentiometric titrations were carried out using a Metrohm Titrando 888 titration instrument in a double-jacketed glass cell. Each solution was stirred continuously, while the temperature was kept at 25.0 ± 0.1 °C by a Julabo F12-MB thermostat. The equilibrium cell potentials were measured by a Jenway 3540 Bench pH and conductivity meter using a SenTiX-62 combined glass electrode (from WTW). The ionic strength was adjusted to 4 M with NaCl.

During the course of electrode calibration, a weak acid (0.200 M malonic acid) and, subsequently, a strong acid (0.196 M HCl) were titrated with ≈1 M NaOH. These titration curves were evaluated with the *pHCali*[25] software. The program applies a nonlinear-fitting procedure, allowing for calculation of the electrode slope and intercept, the pK_w, the first and second protonation constants of the malonate ion, the exact concentration of the titrant, and the carbonate content. For log K_w, a value of −14.26 was used (determined previously by applying a platinized platinum electrode),[16] while the two protonation constants of CO_3^{2-} were taken from the literature.[26]

As a result, the electrode response was found to be linear in the range of 1.8 < pH_c < 12.2, where pH_c is defined as $-\log([H^+]/c^\circ)$. The linear relationship is demonstrated in Figures S1 and S2. Furthermore, the ratio of CO_3^{2-} relative to NaOH was found to be <0.5 mol %, while the slope and intercept (±3SE) were calculated to be 58.1 ± 0.2 and 456.3 ± 1.1 mV, respectively. On the basis of the latter parameter, the error in pH_c is ±0.02, which we consider to be the minimum error of the equilibrium constants determined.

To investigate the protonation of $Gluc^-$, two series were studied: 70 mL solutions containing $[Gluc^-]_T$ = 0.100 and 0.200 M were titrated with 0.246 and 0.496 M HCl solutions, respectively. For component X, hereafter $[X]_{T,0}$ or $[X]_T$ represents its initial total (at V = 0 for titrations) or simply its total concentration (for NMR and IR measurements), while [X] is referred to as the equilibrium concentration.

To study the complex formation between Mg^{2+} and $Gluc^-$ ions, two titration series were undertaken. First, 70 mL solutions with $[Gluc^-]_{T,0}$ = 0.100−0.200 M, $[Mg^{2+}]_{T,0}$ = 0.051−0.203 M, and $[HCl]_{T,0}$ = 0.005 M were titrated with 0.050 M NaOH. Second, 70 mL samples containing $[Gluc^-]_{T,0}$ = 0.100−0.200 M and $[OH^-]_{T,0}$ = 0.005−0.100 M or $[HCl]_{T,0}$ = 0.096 M were titrated with 1.017 M $MgCl_2$.

NMR Spectroscopic Measurements. ^{1}H and ^{13}C NMR spectra were recorded with a Bruker Ascend 500 MHz NMR spectrometer equipped with a 5 mm inverse broad-band probe head furnished with

DOI: 10.1021/acs.inorgchem.9b00289
Inorg. Chem. 2019, 58, 6832−6844

z-oriented magnetic-field-gradient capability. The magnetic field was stabilized by locking it to the ^{2}D signal of the solvent prior to spectral acquisition. The sample temperature was set to 25 ± 1 °C for measurements at a constant temperature and to 7−47 °C during the temperature-dependent experiments. 10% (v/v) D_2O was added to each sample, and 32 or 256 interferograms were collected to obtain the ^{1}H or ^{13}C NMR spectra. For comparison, the spectra were baseline-corrected and normalized.

The pH values of the solutions were set using the SenTix-62 electrode, which was calibrated with buffers (obtained from WTW). Conversely, the activity coefficient of H^+ in the buffers is considerably different from that in the samples because of the more concentrated ionic media and use of D_2O in the latter. Thus, the nominal pH adjusted in the solutions is referred to as pH* hereafter, and its deviation from the real pH can be estimated as ±0.2 units. Nevertheless, this difference is acceptable for qualitative purposes.

To study the complex formation between Mg^{2+} and $Gluc^-$ at neutral pH, solutions with $[Gluc^-]_T$ = 0.200 M and $[Mg^{2+}]_T$ = 0.000−0.492 M were prepared. The ionic strength was adjusted to 4 M. It has to be noted that incidental variations in the pH may affect the chemical shifts of $Gluc^-$. For this series, however, the pH* was found to be 6.7−6.9; thus, the formation of HGluc can be ruled out. Consequently, the observed changes in the chemical shifts were solely due to complex formation.

To study the pH dependence of the spectra, sample sets with $[Gluc^-]_T$ = 0.2 M as well as $[Gluc^-]_T$ = 0.2 M and $[Mg^{2+}]_T$ or $[Ca^{2+}]_T$ = 0.1 M were prepared at pH* = 6−13. The temperature dependence of a solution containing $[Gluc^-]_T$ = 0.2 M and $[Mg^{2+}]_T$ = 0.1 M was studied in the range of 7−47 °C, and the pH* was adjusted to 10.0 at T = 22 °C. In each case, the pH* was set by HCl or NaOH solutions (right before the measurements), and the ionic strength was not adjusted.

IR Spectroscopic Measurements. The IR spectra were recorded at room temperature, using a Bio-Rad Digital Division FTS-65 A/896 Fourier transform infrared instrument with a spectral resolution of 4 cm^{-1}. The measurements were performed in transmittance mode in the 750−4000 cm^{-1} range, and 256 scans were collected for each sample. The spectra were baseline-corrected and normalized.

To investigate the effect of Mg^{2+} ions on the IR absorption of gluconate, a series with $[Gluc^-]_T$ = 0.2 M and $[Mg^{2+}]_T$ = 0−1.0 M was prepared by applying D_2O as the solvent. The pH* values of the solutions were checked and found to be neutral.

COMPUTATIONS

Data Evaluation and Speciation Calculations. The potentiometric and NMR spectroscopic data were evaluated with the aid of *PSEQUAD*.[27] The general complexation reaction and corresponding conditional stability product, β_{pqr}, read as

$$pMg^{2+} + qGluc^- + rH_2O = Mg_pGluc_q(OH)_r^{(2p-q-r)+} + rH^+ \quad (4)$$

$$\beta_{pqr} = \frac{[Mg_pGluc_q(OH)_r^{(2p-q-r)+}][H^+]^r}{[Mg^{2+}]^p[Gluc^-]^q(c^\circ)^{1+r-p-q}} \quad (5)$$

During fitting, the stability product, log β_{pqr}, was refined by minimizing the so-called fitting parameter, FP, which reads as

$$FP = \sqrt{\frac{\sum_{i=1}^{n}(Y_{i,calc} - Y_{i,meas})^2}{n-k}} \quad (6)$$

where $Y_{i,calc}$ and $Y_{i,meas}$ pertain to the calculated and measured data (pH_c or chemical shift), while n and k represent the number of the measured data and fitted parameters, respectively. The log K_w value was set to −14.26[16] throughout the calculations.

For homogeneous systems, speciation calculations were carried out utilizing the *MEDUSA*[28] program. For heterogeneous systems, where the solubility is controlled by $Th(OH)_4(s)$, *PSEQUAD*[27] was applied by setting the $Th(OH)_4(aq)$ complex as the primary species. The stability product of $Th(OH)_4(s)$ and those of the various hydrolysis species, $Th(OH)_r^{(4-r)+}$, were taken from the respective NEA-TDB review.[29] No formation constant was selected for the $Th(OH)_3^+$ complex; hence, it was taken from ref 30. Concerning the gluconate complexes of thorium(IV),[5,6] the equilibrium constants were taken from ref 17. All of these values are presented in Table S1.

In order to perform speciation calculations for the Th^{4+}/Mg^{2+}/$Gluc^-$/OH^- system, the literature data of the thorium(IV)-containing species were converted to I = 4 M. For this purpose, the specific-ion-interaction theory (SIT)[31−34] was applied. The SIT introduces ion-interaction parameters (ε_{ij}) to describe short-range ion interactions and the ionic strength dependence of the mean activity coefficient. It is worth mentioning that, in general, the Pitzer approach[35] or the modified SIT[36] is known to be more accurate at higher ionic strength. The literature data, however, are insufficient (especially for the gluconate complexes) to perform accurate calculations with these models. Nonetheless, the SIT approach was found to be applicable at I > 4 M in numerous cases, a also for different background electrolytes,[37−39] including NaCl.[40,41] Hence, we used this model following the approach of the standard NEA-TDB review.[29]

The respective ε_{ij} coefficients (Table S2) were taken from refs 29 and 42. The stability constants calculated using the SIT equation are listed in Table S1. For further details, the reader is referred to the Supporting Information and to refs 29−34.

Quantum-Chemical Calculations. To model the structure of the complexes, in vacuo calculations were performed using the M11 range-separated hybrid meta-generalized gradient approximation density functional theory (DFT) functional[43] coupled with the cc-pVDZ basis set. The recently developed M11 functional was shown to provide excellent performance for main-group energies, proton and electron affinities, barrier heights, bond dissociation, and noncovalent interaction energies. The computations were coupled with conformational analysis by varying the freely rotating HCCH dihedral angles of $Gluc^-$.

Subsequent geometry optimizations of all structures were carried out utilizing the same functional and the aug-cc-pVTZ basis set. These calculations with the higher basis set were undertaken by taking solvent effects into account with the aid of the conductor-like polarizable continuum model (CPCM)[44] (where water was considered to be the solvent). All calculations were carried out using the *Gaussian09*[45] software package.

RESULTS AND DISCUSSION

Complexation between Mg^{2+} and $Gluc^-$ in a Neutral Medium. With increasing $[MgCl_2]_T$ in solutions containing $[Gluc^-]_T$ = 0.2 M, the H2 and H3 NMR signals of $Gluc^-$ show a gradual downfield shift (Figure 1). Simultaneously, the position of the C1 signal shifts upfield. Such variations indicate complex formation as in the case of Ca^{2+} binding, which was confirmed by 2D ^{1}H−^{43}Ca NMR measurements.[46] Moreover, no additional peaks appear on the spectra, which stems from

DOI: 10.1021/acs.inorgchem.9b00289
Inorg. Chem. 2019, 58, 6832−6844

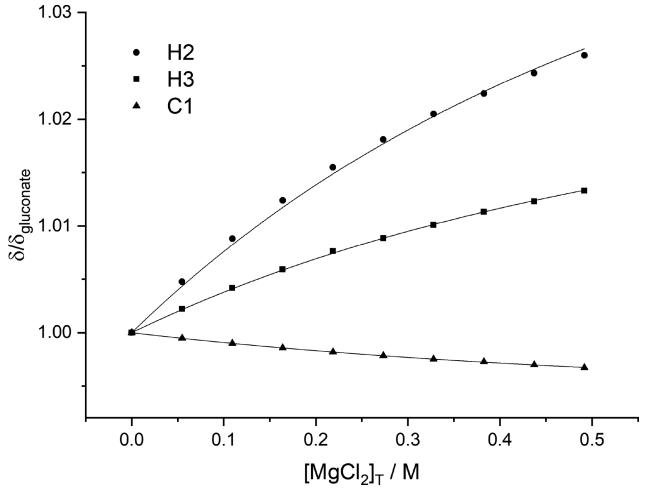

Figure 1. ^{1}H and ^{13}C NMR chemical shifts as a function of $[Mg^{2+}]_T$. Experimental conditions: I = 4 M (NaCl) and T = 25 ± 1 °C; $[Gluc^-]_T$ = 0.200 M. Symbols represent measured data, while solid lines were calculated assuming the formation of $MgGluc^+$. The chemical shifts were normalized to the neat $Gluc^-$ ion for better visualization.

fast ligand-exchange processes between free and complexed $Gluc^-$.

The experimentally obtained chemical shifts were fitted as a function of $[Mg^{2+}]_T$, assuming formation of the 1:1 complex.[18] The relationship between the observed chemical shift (δ_{obs}) and the equilibrium concentrations of $Gluc^-$ and $MgGluc^+$ is as follows:

$$\delta_{obs} = \frac{\delta_{Gluc^-}[Gluc^-] + \delta_{MgGluc^+}[MgGluc^+]}{[Gluc^-]_T} \quad (7)$$

where δ_{Gluc^-} and δ_{MgGluc^+} are the limiting chemical shifts of $Gluc^-$ and $MgGluc^+$, respectively.

When solely the ^{13}C chemical shifts are fitted, log β_{110} was determined to be 0.25−0.33, with FP (eq 6) being 0.002−0.006 ppm. When only the ^{1}H chemical shifts are fitted, log β_{110} ranged from 0.46 to 0.60 (FP = 0.0006−0.0012 ppm). When both the ^{1}H and ^{13}C shifts were taken into account, log β_{110} was found to be 0.25 on average (FP = 0.002 ppm). The best fitting from each set is shown in Table 1, while the calculations considering all chemical shifts are depicted in Figure 1.

The difference in the formation constants obtained by ^{1}H and ^{13}C nuclei is not unusual for weak complexes because β_{110} and the actual limiting chemical shifts are highly correlated. Hence, on the basis of the NMR results, we suggest 0.4 ± 0.2 for log β_{110}; this value is in reasonable agreement with log β_{110} = 0.70 determined potentiometrically at I = 0.2 M.[18] Using log β_{110} = 0.4, 50% of the ligand molecules are complexed at the highest $[MgCl_2]_T$ (Figure S3).

Although the uncertainty of the formation constant of $MgGluc^+$ is rather high, it seems to be less stable than $CaGluc^+$. This difference is unambiguous in Cannan and Kibrick's work: they determined log β_{110} = 0.70 for $MgGluc^+$ and 1.21 for $CaGluc^+$.[18] In general, the stability order of 1:1 complexes forming between alkaline-earth metal and glycolate, lactate, or glycerate ions is as follows: $Mg^{2+} < Ca^{2+} > Sr^{2+} > Ba^{2+}$.[18,50,51] From Ca^{2+} to Ba^{2+}, the decreasing order follows from the decreasing charge density of the cation.

Table 1. Stability Products, log β_{pqr}, for Equilibria Taking Place in the $Mg^{2+}/Gluc^-/H_3O^+/OH^-$ System[a]

reaction	log β_{pqr} ± 3SE	method[b]	ref
$H_2O = H^+ + OH^-$	−14.26	H_2-Pt POT	16
$HGluc = Gluc^- + H^+$	−3.73 ± 0.05	GLE POT	p.w.
$Gluc^- = GlucH_{-1}^{2-} + H^+$	−13.92 ± 0.06	GLE POT	p.w.
	−14.08 ± 0.03	H_2-Pt POT	16
	−13.90 ± 0.03	^{13}C NMR	16
$Mg^{2+} + H_2O = MgOH^+ + H^+$	−12.33 ± 0.18	GLE POT	47
$Ca^{2+} + H_2O = CaOH^+ + H^+$	−13.92 ± 0.36	ISE POT	48
$Mg(OH)_2(s) + 2H_2O = Mg^{2+} + 2H^+$	17.64 ± 0.20[c,d]	SOL/ICP-OES	49
$Ca(OH)_2(s) + 2H_2O = Ca^{2+} + 2H^+$	24.00 ± 0.09[c]	ISE POT	48
$Mg^{2+} + Gluc^- = MgGluc^+$	0.47 ± 0.05	^{1}H NMR	p.w.
	0.25 ± 0.02	^{13}C NMR	p.w.
	0.25 ± 0.05	^{1}H/^{13}C NMR	p.w.
	0.33 ± 0.04	GLE POT	p.w.
	0.4 ± 0.2[e]		p.w.
	0.70[d]	GLE POT	18
$Ca^{2+} + Gluc^- = CaGluc^+$	0.85 ± 0.15	^{13}C NMR	46
	1.21[d]	GLE POT	18
$Mg^{2+} + Gluc^- + H_2O = MgGlucOH^0 + H^+$	−10.20 ± 0.01	GLE POT	p.w.
$Ca^{2+} + Gluc^- + H_2O = CaGlucOH^0 + H^+$	−11.73 ± 0.03	H_2-Pt POT	16
$Mg^{2+} + Gluc^- + 2H_2O = MgGluc(OH)_2^- + 2H^+$	−21.66 ± 0.06	GLE POT	p.w.
$3Mg^{2+} + 2Gluc^- + 4H_2O = Mg_3Gluc_2(OH)_4^0 + 4H^+$	−38.52 ± 0.10	GLE POT	p.w.
$3Ca^{2+} + 2Gluc^- + 4H_2O = Ca_3Gluc_2(OH)_4^0 + 4H^+$	−43.80 ± 0.03	H_2-Pt POT	16

[a]For comparison, analogous constants for the $Ca^{2+}/Gluc^-/H_3O^+/OH^-$ system are presented. The constants correspond to T = 25 °C and I = 4 M (NaCl), unless indicated differently. [b]H_2-Pt, GLE, ISE POT: potentiometry applying hydrogen (platinized platinum), glass or calcium ion-selective electrode. ^{1}H and ^{13}C NMR: nuclear magnetic resonance spectroscopy. SOL/ICP-OES: solubility determined with inductively coupled plasma optical emission spectroscopy. [c]Here the solubility product (log K_{sp}) is given. [d]The experiments were performed at T = 22.5 °C in ref 49 and at I = 0.2 M (KCl) in ref 18. [e]Recommended value for log β_{110} (see the text for discussion).

Conversely, other thermodynamic factors may play important roles in the complex formation reactions of Mg^{2+}. First, Mg^{2+} prefers 6-fold coordination, while the first coordination sphere of Ca^{2+} is rather flexible, with the hydration number being 6−8.[52−59] As a result, binding of the COO^- group requires the loss of (at least) one solvent molecule for Mg^{2+}, while Ca^{2+} can accommodate it without dehydration, yielding more stable calcium(II) complexes. Moreover, if dehydration occurs in both cases, it is again more favorable for Ca^{2+}: the enthalpy of dehydration was found to be 16.8−17.7 kJ·mol^{-1} for $Ca(H_2O)_7^{2+}$, while 23.4−24.2 kJ·mol^{-1} was determined for $Mg(H_2O)_6^{2+}$.[60]

It is important to note that the release of water molecules would result in higher disorder, thereby favoring the formation of $MgGluc^+$. The higher stability constant of $CaGluc^+$, however, indicates that enthalpy effects dominate the formation of 1:1 complexes.

Coordination Mode of $Gluc^-$ in the $MgGluc^+$ Complex. The variations of the NMR chemical shifts do not allow one to decide whether $Gluc^-$ is bound in a mono- or

DOI: 10.1021/acs.inorgchem.9b00289
Inorg. Chem. 2019, 58, 6832−6844

a bidentate manner to the metal ion. To unravel the coordination mode in the 1:1 complex, a solution series of $[Gluc^-]_T$ = 0.2 M and $[Mg^{2+}]_T$ = 0−1 M was studied via IR spectrosopy, applying D_2O as the solvent.

Upon the addition of Mg^{2+} ions, the region of O−H stretching vibrations (3000−3700 cm^{-1}) does not exhibit any significant changes upon metal-ion coordination. In conclusion, the metal−ligand interactions are localized to the region of carboxylate stretching vibrations, in agreement with a previous IR study.[19] Therefore, only this region is presented (Figure 2) and discussed.

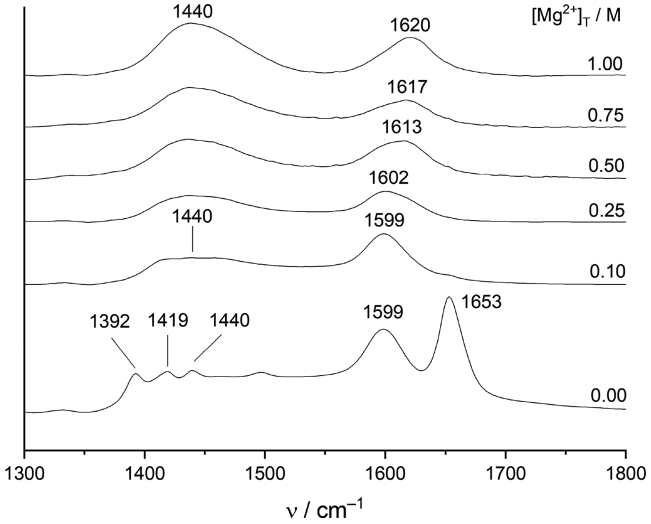

Figure 2. Traces of IR spectra of a solution series of $[NaGluc]_T$ = 0.2 M and $[MgCl_2]_T$ = 0−1 M at room temperature.

Assignment of the symmetric and asymmetric stretching vibrations of $Gluc^-$ is rather difficult. The asymmetric vibration mode is obviously split into two components (1599 and 1653 cm^{-1}), which was also previously observed on the spectrum of the solid NaGluc salt.[16] Such a splitting is an indicative of two different coordination modes between the metal ion and ligand, as was proposed for the cobalt(II) acetate dihydrate and calcium succinate trihydrate salts.[61,62] Conversely, given that Na^+ is a weekly binding cation, the degree of association between Na^+ and $Gluc^-$ is probably low; therefore, it cannot completely account for the observed splitting. An analogous interpretation can be the dynamic equilibrium between the planar and bent-chain conformations of the free ligand;[20−23] however, none of these two scenarios can be unambiguously confirmed or ruled out. Nevertheless, the symmetric vibration mode must be split as well, giving rise to the appearance of two peaks in the region of 1350−1450 cm^{-1}. Furthermore, this region coincides with the C−O−H bending modes,[19,63] which explains the presence of a third peak in this frequency range.

Upon the addition of Mg^{2+} ions, the spectra simplify to two broad peaks, known as the symmetric and asymmetric COO^- regions.[63−65] Two important conclusions can be drawn from the observed variations. First, the disappearance of the splitting seen for $Gluc^-$ implies one coordination mode. Second, the distance between the peak maxima of the symmetric and asymmetric modes increases with increasing $[Mg^{2+}]_T$, as a token of complex formation. At $[MgCl_2]_T$ = 1 M, ca. 70% of the ligand is bound in the 1:1 complex, where the distance is 180 cm^{-1}. On the basis of IR analysis of numerous solid complexes,[64,65] such a difference refers to the so-called pseudobridged monodentate coordination, where one oxygen atom of the COO^- group is bound to the metal ion, while the other establishes hydrogen bonding of a neighboring OH group.

Solely on the basis of the IR spectra, participation of the OH groups in ligand coordination is still uncertain. To address this problem, quantum-chemical computations were undertaken. The following scenarios were taken into consideration: (1) monodentate binding, (2) bidentate coordination of COO^-, and (3) monodentate binding of COO^- and the adjacent OH group. During calculations, octahedral geometry around Mg^{2+} was assumed.

For bidentate coordination modes, the binding of both oxygen atoms of the COO^- group (Figure S4) yields a less stable complex than monodentate coordination of both the COO^- and OH groups (Figure S5). The difference in energy is 13.5 kJ·mol^{-1}, significantly higher than the energy of thermal motion (≈2.5 kJ·mol^{-1} at 25 °C). Thus, bidentate coordination of COO^- can be excluded, in agreement with the outcome of the IR experiments.

To compare the stabilities of the chelate (Figure S5) and monodentate species, the number of water molecules must match. Hence, a water molecule was added to the chelate complex, and its position was varied around the metal ion and along the gluconate backbone. The most stable structure is depicted in Figure S6. Alternatively, this complex represents the product of the reaction

$$Mg(H_2O)_5Gluc^+ = Mg(H_2O)_4Gluc^+ + H_2O \quad (8)$$

Its energy, however, is higher by 6.2 kJ·mol^{-1} than that of $Mg(H_2O)_5Gluc^+$ (Figure S7). In conclusion, the bidentate coordination of $Gluc^-$ is not favored because of the strong hydration of Mg^{2+}. Additionally, one oxygen atom of COO^- establishes strong hydrogen bonding with an axial metal-bound water molecule (dashed line in Figure S7), resulting in pseudobridged monodentate coordination.[64,65] The discussion of the role of hydrogen bonding is deferred to the Role of Hydrogen Bonds in the $MgGluc^+$ and $MgGlucOH^0$ Complexes section.

In summary, both IR measurements and structure computations suggest that $Gluc^-$ acts as a monodentate ligand in the $MgGluc^+$ complex. Conversely, chelate formation is preferred for $CaGluc^+$.[46]

Effect of the pH on the Complexation between Mg^{2+} and $Gluc^-$ Ions. In order to examine the complex formation between Mg^{2+} and $Gluc^-$ as well as protonation of the ligand, a series of potentiometric titrations were performed in the pH_c range of 1.9−12.1. To demonstrate the pH changes caused by complex formation, several comparative titration curves are shown in Figure 3.

The red curve depicts the pH_c values of a slightly acidic solution of 0.2 M NaGluc titrated with NaOH. Upon the addition of $MgCl_2$ (0−0.2 M), the shapes of the curves resemble that of 0.2 M NaGluc. The pH_c, however, is much lower after the equivalence point, indicating complex formation.

Furthermore, the titration curves of solutions with $[Gluc^-]_{T,0}$ = 0.1 M and $[Mg^{2+}]_{T,0}$ = 0.1 M (orange curve) and $[Gluc^-]_{T,0}$ = 0.2 M and $[Mg^{2+}]_{T,0}$ = 0.05 M (blue curve) are essentially the same in the alkaline region. According to the Guldberg−Waage mass action law, the equilibrium concentration of the complex(es) formation must be proportional to

DOI: 10.1021/acs.inorgchem.9b00289
Inorg. Chem. 2019, 58, 6832−6844

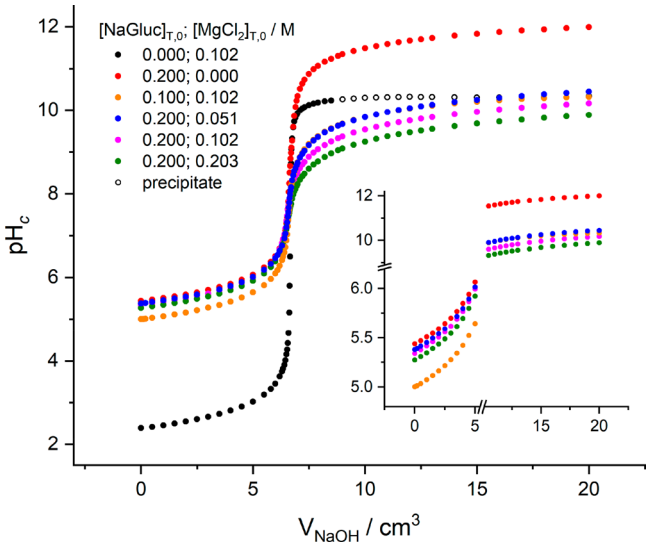

Figure 3. Equilibrium pH_c values as a function of the added titrant volume. Experimental conditions: T = 25 ± 1 °C, I = 4 M (NaCl), and V_0 = 70 mL; $[HCl]_{T,0}$ = 0.005 M, while $[Gluc^-]_T$ and $[Mg^{2+}]_T$ are listed in the legend. The titrant was 0.050 M NaOH in each case. Hollow circles indicate the range of precipitation of $Mg(OH)_2(s)$. Inset: Zoomed region of the acidic and alkaline pH regimes.

that of $[Mg^{2+}]^{\alpha}\cdot[Gluc^-]^{\beta}$ and, hence, to that of $[Mg^{2+}]_T^{\alpha}\cdot[Gluc^-]_T^{\beta}$. Because in both cases $[Mg^{2+}]_T\cdot[Gluc^-]_T \approx 0.01$, the similar values of pH_c imply that $\alpha = \beta = 1$, i.e., the formation of 1:1 species. It is also worth mentioning that, with increasing $[Mg^{2+}]_{T,0}$, a small but significant decrease in pH_c is discernible in the acidic region, which follows from the reaction

$$Mg^{2+} + HGluc = MgGluc^+ + H^+ \quad (9)$$

When the titration curve of the solution containing only 0.1 M $MgCl_2$ (black curve) is compared to those containing $Gluc^-$, it is seen that the increase of pH_c is less steep for the latter, indicating a stronger buffering capacity and, thus, complexation between the Mg^{2+} and $Gluc^-$ ions in the alkaline regime. This is strongly supported by the fact that, in contrast to the solution with 0.1 M $MgCl_2$, precipitation of $Mg(OH)_2(s)$ cannot be observed in the presence of $Gluc^-$.

Expectedly, titrations performed with 1 M $MgCl_2$ as the titrant (Figure S8) exhibit a remarkable pH_c decrease (ΔpH_c = 2) upon the addition of 5 mL of titrant. Starting with the titrations from the acidic region ($[HCl]_{T,0}$ = 0.1 M), a lower but still pronounced pH_c decrease ($\Delta pH_c \approx 0.3$) is seen as a token of the formation of $MgGluc^+$ (eq 9).

During data evaluation, the pH- and $MgCl_2$-dependent titrations as well as the protonation measurements of $Gluc^-$ were fitted simultaneously. Assuming the formation of HGluc, $GlucH_{-1}^{2-}$, $MgGluc^+$, and its two deprotonated forms, $MgGluc(OH)^0$ and $MgGluc(OH)^{2-}$, the FP was found to be 0.024 (in pH_c units).

Further improvement of the FP (0.017) could be achieved by taking the formation of $Mg_3Gluc_2(OH)_4^0$ into consideration. Expectedly, the two curves, starting from the alkaline region and with $MgCl_2$ as the titrant, are the most affected ones. That is, the individual FP decreased from 0.034 to 0.021 (Figure S8, red curve) as well as from 0.040 to 0.015 (Figure S8, blue curve). Given that the calcium(II) analogues were detected in the presence of $Gluc^-$,[15,16] the presence of such a trinuclear magnesium(II) complex seems to be realistic.

In conclusion, the proposed chemical model for the $Mg^{2+}/Gluc^-/OH^-/H^+$ system consists of HGluc, $GlucH_{-1}^{2-}$, $MgGluc^+$, $MgGlucOH^0$, $MgGluc(OH)_2^-$, and $Mg_3Gluc_2(OH)_4^0$. The calculated potentials are depicted in Figures S8–S10, while the respective stability products are listed in Table 1. To the best of our knowledge, the deprotonation constant of HGluc (at I = 4 M NaCl) is the only one to date. Regarding $GlucH_{-1}^{2-}$, the reliability of its stability constant (−13.92) is justified by the excellent agreement with that (−13.90) determined previously via ^{13}C NMR at the same ionic strength.[16] As for $MgGluc^+$, $\log \beta_{110}$ = 0.33 agrees well with that proposed from the NMR results (0.4 ± 0.2).

Comparing the stability products of the calcium(II) and magnesium(II) analogues (i.e., the 1:1:1 and 3:2:4 species), it is evident that more stable complexes are formed with Mg^{2+}. This striking difference can be explained by the fact that Mg^{2+} ions undergo hydrolysis more readily. In fact, the stability of $MgOH^+$ is higher by roughly 1.5 orders of magnitude than that of $CaOH^+$.[47,48] Similarly, the solubility product of $Mg(OH)_2(s)$ is smaller by more than 6 orders of magnitude than that of $Ca(OH)_2(s)$.[48,49]

Figure 4 shows the concentration distribution diagram of magnesium(II) for the most concentrated solution used in our

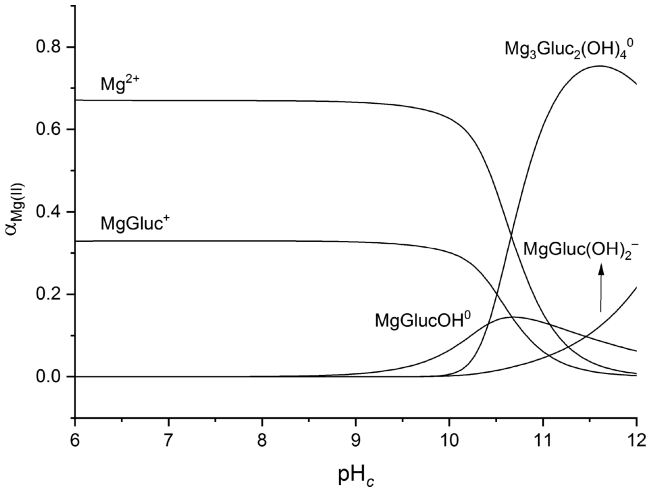

Figure 4. Speciation diagram with respect to magnesium(II) as a function of pH_c. The calculations were based on equilibrium constants corresponding to T = 25 °C and I = 4 M (NaCl). Total concentrations: $[Mg^{2+}]_T$ = 0.100 M and $[Gluc^-]_T$ = 0.200 M.

studies ($[Gluc^-]_T$ = 0.2 M and $[Mg^{2+}]_T$ = 0.1 M). It is seen that the $Mg_3Gluc_2(OH)_4^0$ species is the predominant one in the pH_c range of 10.5–12.0. As for the stoichiometry of $Mg_3Gluc_2(OH)_4^0$, it shows a pronounced similarity with both the $Mg_3(OH)_4^{2+}$ and $Mg_4(OH)_4^{4+}$ polynuclear species that were invoked in previous studies.[47,66,67] These complexes, however, were not accepted in a later critical review[68] because their formation coincides with the onset of the precipitation of $Mg(OH)_2(s)$. Nevertheless, the formation of $Mg_3Gluc_2(OH)_4^0$ can be indirect evidence of the existence of these hydroxido complexes because they might be stabilized by $Gluc^-$ through the following reactions:

$$Mg_3(OH)_4^{2+} + 2Gluc^- = Mg_3Gluc_2(OH)_4^0 \quad (10)$$

DOI: 10.1021/acs.inorgchem.9b00289
Inorg. Chem. 2019, 58, 6832–6844

$$Mg_4(OH)_4^{4+} + 2Gluc^- = Mg_3Gluc_2(OH)_4^0 + Mg^{2+} \quad (11)$$

Effect of $MgCl_2$ on the Solubility of Thorium(IV). The impact of $MgCl_2$ on the solubility of $Th(OH)_4(s)$ in the presence of $Gluc^-$ was assessed via calculation of the solubility curve of thorium(IV) using the solubility and stability products listed in Tables 1 and S1. The pH_c ranged from 7 to 10, $[Gluc^-]_T$ was set to 10^{-5} to 10^{-2} M, and $[Mg^{2+}]_T$ was adjusted to 0, 0.1, 0.2, 0.3, 0.5, and 1 M. It has to be mentioned that the last two concentrations are too high compared to that of the background electrolyte; therefore, the ionic interaction coefficients (Table S2) are only approximate. Thus, these calculations are considered to be semiquantitative.

It is known that thorim(IV) has a high affinity to form multinuclear hydroxido complexes. For the formation of these species, however, reasonably high concentrations of thorium(IV) (>10^{-6} M) and acidic solutions (pH < 5) are prerequisites.[29,30,68] Given the pH range of the present simulations, these complexes were neglected. Furthermore, because of the presence of $MgCl_2$, precipitation of $Mg(OH)_2(s)$ is expected to occur. The only literature data with respect to 4 M NaCl was obtained by the solubility method at 22.5 °C.[49] Although it was later not accepted in Ekberg and Brown's critical review, it was used here to estimate the onset of precipitation.

Figure 5 shows the solubility curve of thorium(IV) in the absence and presence of 10^{-5} M NaGluc and the increasing amount of $MgCl_2$. At $[MgCl_2]_T$ = 0 M and pH_c < 9, $\log([Th^{IV}]_T/c^o)$ increases by 0.1−0.2 units because of the $ThGluc(OH)_4^-$ complex.[5,6,17] The increase is significantly higher at pH_c = 10, where the $ThGluc(OH)_5^{2-}$ (or the $ThGlucH_{-1}(OH)_4^{2-}$) complex[5,17] is formed to a significant extent.

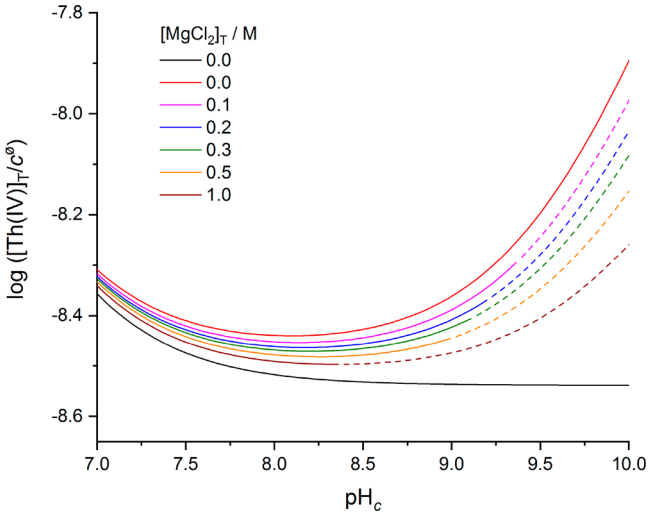

Figure 5. Solubility of thorium(IV) hydroxide as a function of pH_c. The calculations were based on equilibrium constants corresponding to T = 25 °C and I = 4 M (NaCl). Total concentrations: $[Gluc^-]_T$ = 0 M (black line) and 0.00001 M (colored lines). $[Mg^{2+}]_T$: listed in the legend. In the pH ranges depicted with dashed lines, $Mg(OH)_2(s)$ is expected to precipitate.

Increasing $[MgCl_2]_T$ lowers the solubility of thorium(IV) dramatically because of the formation of magnesium(II) gluconate complexes proposed in this work (Table 1). That is, at high concentrations of $MgCl_2$, their formation partially suppresses that of the thorium(IV) gluconate species. The direction of this variation would be the opposite if a ternary complex such as $CaThGluc_2(OH)_4^0$ was also formed with Mg^{2+}. This kind of species, however, was not reported so far.

At higher concentrations of gluconate (Figures 6 and S11 and S12), however, the decrease of the solubility becomes less pronounced, which stems from the extremely high stability of both the $ThGluc(OH)_4^-$ and $ThGluc(OH)_5^{2-}$ species. For instance, at pH_c = 7, $\log([Th^{IV}]_T/c^o)$ is −8.3 at $[Gluc^-]_T$ = 0 M, while it increases to −6.3 at $[Gluc^-]_T$ = 0.01 M (Figure 6). Upon the addition of 1 M $MgCl_2$, this value decreases only to −6.8. In conclusion, the formation of thorium(IV) gluconate complexes cannot be completely suppressed even at high $[Mg^{2+}]_T/[Gluc^-]_T$ ratios. On the other hand, the effect of the Mg^{2+} ions might be expected to be more significant under the conditions of radioactive waste disposals, with $[MgCl_2]_T$ being as high as 4 M.[3]

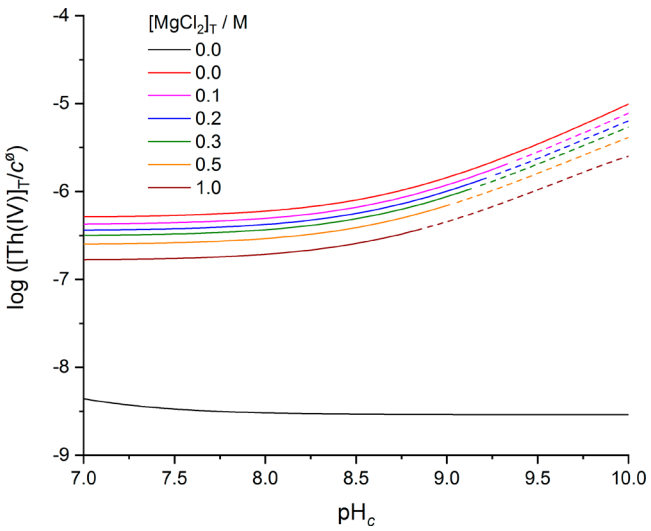

Figure 6. Solubility of thorium(IV) hydroxide as a function of pH_c. The calculations were based on equilibrium constants corresponding to T = 25 °C and I = 4 M (NaCl). Total concentrations: $[Gluc^-]_T$ = 0 M (black line) and 0.01 M (colored lines). $[Mg^{2+}]_T$: listed in the legend. In the pH ranges depicted with dashed lines, $Mg(OH)_2(s)$ is expected to precipitate.

As any speciation model, this one should also be justified experimentally via solubility measurements, albeit carrying out such experiments in the alkaline pH range is a difficult endeavor even for the experts of this field. First, solubility equilibria of actinide hydroxides are usually established very slowly (if at all) because of the formation of more soluble amorphous precipitates or amorphous layers on the surface of the thermodynamically stable, crystalline phases.[30] Namely, the transformation of such metastable phases to crystalline phases is kinetically hindered. Second, because the concentrations to be detected are extremely low (<10^{-8}−10^{-7} M), the scattering range of the data is often 1 order of magnitude or higher, even upon application of state-of-the art instrumentation. The predicted effects of $MgCl_2$ are within this uncertainty and, hence, difficult to detect experimentally. Thus, we believe that our calculations serve as a good first estimation for modeling the solubility of thorium(IV) in the presence of NaGluc and $MgCl_2$.

DOI: 10.1021/acs.inorgchem.9b00289
Inorg. Chem. 2019, 58, 6832−6844

Effect of the pH and Temperature on the NMR Spectra of $Gluc^-$ in the Presence of $MgCl_2$. To gain further insights concerning the structures of the complexes formed, a series of NMR spectra were recorded. Figure 7

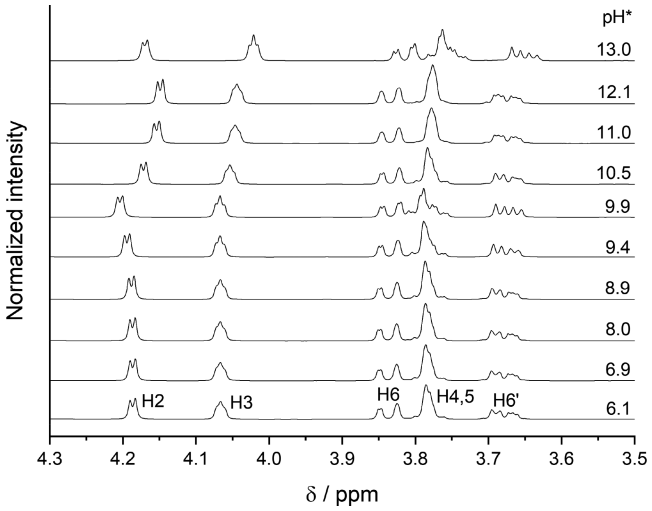

Figure 7. ^1H NMR spectra of solutions containing $[Gluc^-]_T$ = 0.200 M and $[Mg^{2+}]_T$ = 0.100 M as a function of the nominal pH* at T = 25 ± 1 °C.

shows the pH dependence of the ^1H spectra of $Gluc^-$ in solutions containing $[Gluc^-]_T$ = 0.2 M and $[Mg^{2+}]_T$ = 0.1 M. At pH* = 6, ca. 14% of $[Gluc^-]_T$ is bound in the $MgGluc^+$ complex. [It has to be noted that only a semiquantitative comparison is possible because the formation constants of the present samples are somewhat different (I < 1 M) from those used for the speciation calculations (I = 4 M).]

At pH* = 6–9, the spectra remain unchanged, while at pH* = 9.5–10, the H2 peak is shifted slightly downfield; furthermore, the H4–H5 signals become more resolved. These minor variations probably result from the formation of $MgGlucOH^0$, which is supported by the speciation diagram (Figure 8): the formation of this species starts at pH_c = 9.

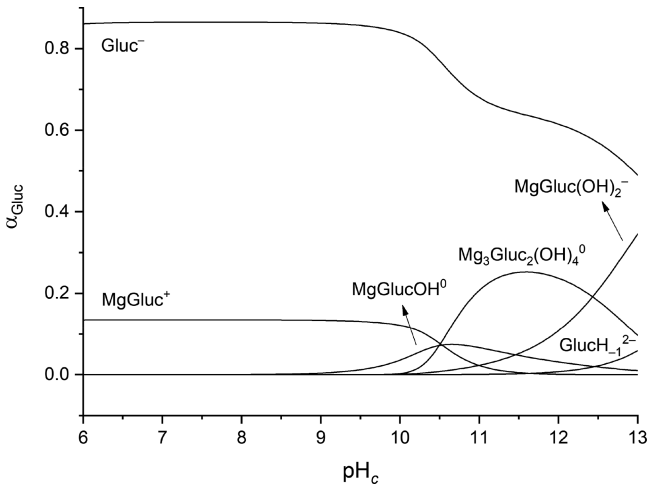

Figure 8. Speciation diagram with respect to gluconate as a function of pH_c. The calculations were based on equilibrium constants corresponding to T = 25 °C and I = 4 M (NaCl). Total concentrations: $[Mg^{2+}]_T$ = 0.100 M and $[Gluc^-]_T$ = 0.200 M.

Interestingly, the shape of the spectra above pH* = 10 returns to those observed at pH* < 9. This is a hint that another complex is formed that suppresses the formation of $MgGlucOH^0$. Indeed, these reverse spectral changes coincide well with the $Mg_3Gluc_2(OH)_4^0$ species, which appears at pH_c = 10 and becomes the dominant one up to pH_c = 12 (Figure 8). In parallel, the amount of free ligand drops to approximately 60%, yet the spectra resemble those of the free ligand (at pH* = 6). This similarity implies that the interactions between Mg^{2+} and $Gluc^-$ are weaker in the trinuclear complex than in $MgGlucOH^0$; hence, $Mg_3Gluc_2(OH)_4^0$ might be the ligand-stabilized form of the $Mg_3(OH)_4^{2+}$ or $Mg_4(OH)_4^{2+}$ unit.[47,66,67]

Above pH* ≈ 13, the H3–H6′ peaks are slightly shifted upfield because of the formation of $GlucH_{-1}^{2-}$. Conversely, the same downfield shift is seen on the H2 signal, indicating that the structures of the $MgGlucOH^0$ and the newly-formed $MgGluc(OH)_2^-$ species are similar. This conclusion is corroborated by the ^{13}C NMR spectra as well (Figure S13), on which the same trend is seen. Additionally, the C1 signal (Figure S14) exhibits the highest variation: its chemical shift increases by 0.8 ppm at pH* = 10, while it merges to the baseline at pH* = 13. Hence, the COO^- group is likely to be bound to Mg^{2+} in these complexes, similarly to $MgGluc^+$.

On the other hand, it is not obvious where the deprotonation takes place: on an alcoholic OH group of the ligand or on a coordinated water molecule. Although potentiometry is in general not suitable to distinguish between these processes, comparing pK values of the ligand and aqua complexes of a given metal ion might help. In this respect, Van Duin and co-workers proposed a general ionization scheme for the complexation reactions occurring between metal ions and poly(hydroxycarboxylates).[69] Accordingly, deprotonation of $MGluc^+$ can be attributed to ionization of the α-hydroxy (C2–OH) group because the respective pK is lower by ≈2 units than that of the first hydrolytic step of the aqua complex (pK_h). The same conclusion was drawn by analyzing the formation constants of the gluconate complexes of aluminum(III)[70,71] and praseodymium(III),[72] respectively. This so-called metal-ion-induced ligand deprotonation is driven by the formation of very stable, five-membered chelate complexes.

The pK_h of the Mg^{2+} aqua ion (i.e., $-\log \beta_{101}$) was reported to be 12.33.[47] For $MgGluc^+$, using $\log \beta_{110}$ = 0.33, pK_1 is 10.53 (i.e., $\log \beta_{110} - \log \beta_{111}$), while p$K_2$ is 11.46 (i.e., $\log \beta_{111} - \log \beta_{112}$). Given that p$K_1$ < pK_2 < pK_h, even the second deprotonation of the 1:1 complex can occur on the alcoholic OH groups of $Gluc^-$. Because displacement of an alcoholic proton has already been established for the calcium(II) gluconate complexes,[15] comparative NMR measurements were undertaken for the $Gluc^-$, $Mg^{2+}/Gluc^-$, and $Ca^{2+}/Gluc^-$ systems. The ^1H NMR spectra are displayed in Figure 9, while the ^{13}C NMR spectra are depicted in Figures S15 and S16.

From pH* = 6 to 10, only small spectral variations are discernible for both metal-ion-containing solutions compared to the spectra of free $Gluc^-$. These changes are caused by formation of the mononuclear species, discussed in detail in the previous sections as well as in ref 46. Conversely, the spectrum of the $Ca^{2+}/Gluc^-$ system exhibits salient changes at pH* = 12. That is, the ^1H peaks are broadened, especially the H2 and H3 ones, indicating their substantial role in the formation of two deprotonated complexes, $CaGlucOH^0$ and $Ca_3Gluc_2(OH)_4^0$, which is visualized on the distribution diagram of this system (Figure S17). (To calculate the species

DOI: 10.1021/acs.inorgchem.9b00289
Inorg. Chem. 2019, 58, 6832–6844

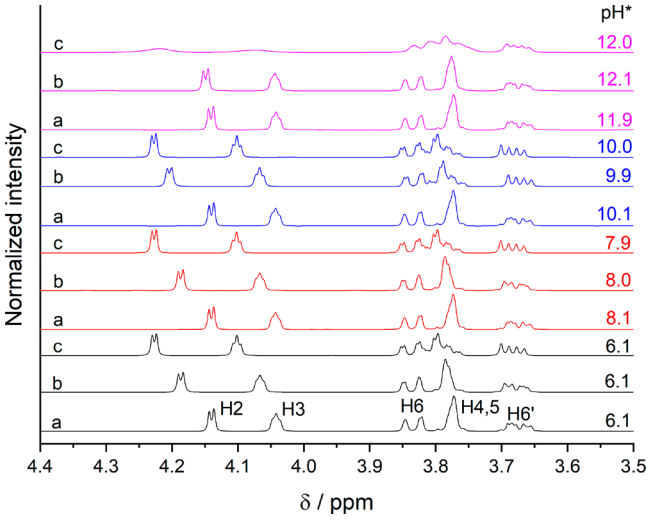

Figure 9. ^{1}H NMR spectra of solutions containing (a) $[Gluc^{-}]_T$ = 0.200 M, (b) $[Gluc^{-}]_T$ = 0.200 M and $[Mg^{2+}]_T$ = 0.100 M, and (c) $[Gluc^{-}]_T$ = 0.200 M and $[Ca^{2+}]_T$ = 0.100 M as function of the nominal pH* at T = 25 ± 1 °C.

distribution, formation constants were obtained from refs 16, 46, and 48.) The dramatic changes seen on the ^{1}H NMR spectra appear on the ^{13}C NMR spectra as well: the peaks of C1−C4 are merged to the baseline, while those of C5 and C6 are widened (Figures S15 and S16).

Such marked changes can be interpreted in terms of metal-ion-induced ligand deprotonation. Namely, the simultaneous coordination of Ca^{2+} and deprotonation of the OH group(s) lead to the formation of alcoholate binding site(s) and therefore much stronger coordinative bonds than those present in the $CaGluc^{+}$ species. As a result, the rate of ligand exchange between bound and free $Gluc^{-}$ slows down, becoming commensurate to the NMR relaxation rates. This, in turn, results in an increase of the signal half-widths, especially of those belonging to the coordination sites. Such a spectral feature was detected for the $Ca^{2+}/Gluc^{-}$ system, and the shift from slow to fast complexation dynamics was attested by temperature-dependent measurements.[15]

Conversely, only marginal changes can be observed for Mg^{2+} at the same pH*. Given that the concentrations of the magnesium(II) gluconate complexes are higher than those of the calcium(II) complexes (Figure 8 vs Figure S17), this difference is striking. Obviously, there is no sign of metal-ion-promoted deprotonation of $Gluc^{-}$, indicating that, similarly to $MgGluc^{+}$, the alcoholic OH groups are not directly bound to the metal ion. The lack of ligand deprotonation is also supported by the temperature-dependent ^{1}H and ^{13}C NMR experiments (Figures S18−S20). At pH* = 10 (at T = 22 °C), where the concentration of $MgGlucOH^{0}$ is the highest, the characteristic transition between the slow and fast exchange rates is absent. Furthermore, the monotonous shift of the C6 peak position provides no sound evidence of coordination of the C6−OH group, which was proposed in a previous ^{13}C NMR relaxation study.[20] A possible reason is that the chemical shift is a less sensitive quantity compared to the relaxation time.

In conclusion, deprotonation in the magnesium(II) gluconate species takes place not on the ligand side but on one of the coordinated water molecules. Still, proton displacement occurs more readily in the $MgGluc^{+}$ complex ($pK_1 \approx 10.5$) than in the $Mg(H_2O)_6^{2+}$ aqua ion ($pK_h \approx 12.3$).[47] Hence, this apparent ligand-promoted hydrolysis of Mg^{2+} in the 1:1 species probably arises from other structural features that are invisible for NMR spectroscopy.

Role of Hydrogen Bonds in the $MgGluc^{+}$ and $MgGlucOH^{0}$ Complexes. The structure of $MgGluc^{+}$ was optimized by assuming octahedral coordination geometry around Mg^{2+} and monodentate binding of the COO^{-} group. The optimum geometry is depicted in Figure 10, while the metal−oxygen distances and hydrogen bonds are listed in Table 2.

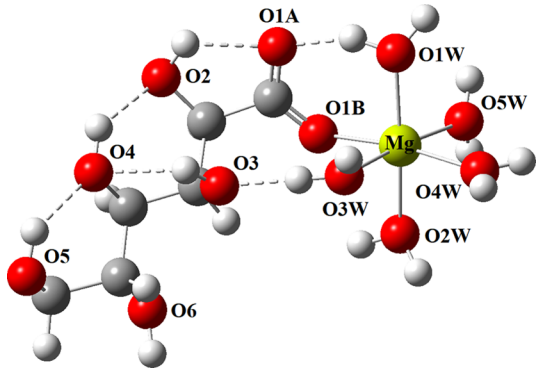

Figure 10. Optimized structure of the $Mg(H_2O)_5Gluc^{+}$ complex at the M11 level, applying the aug-cc-pVTZ basis set. The solvation effects were taken into account by utilizing the CPCM. Dashed lines indicate the hydrogen-bonding system.

First, it is seen that the Mg−O1B distance (2.04 Å) is lower only by 0.03−0.05 Å than the respective Mg−O1W bond lengths, implying that the $Mg^{2+}-{}^{-}OOC$ and $Mg^{2+}-OH_2$ interactions are of similar strengths. Second, two OH groups of $Gluc^{-}$ interact with the hydrating water molecules; namely, very strong hydrogen bonds are established between O1A and O1W (1.69 Å) as well as O3 and O3W (1.75 Å). (In general, strong hydrogen bonds are considered when d < 2.5 Å.[73]) Meanwhile, the respective O1W−H and O3W−H covalent bond lengths are more elongated (0.99−1.00 Å) than those for the other water molecules (≈0.96 Å). Interestingly, those structures that are less stable but whose differences in energy are lower than the energy of thermal motion (≈2.5 kJ·mol^{-1} at 25 °C) exhibit the same coordination motif.

Structure optimization of the $MgGlucOH^{0}$ species was based on the most stable geometry of $MgGluc^{+}$ as the input, and the site of deprotonation was varied from O1W to O5W. The lowest-energy complex is shown in Figure 11, and the corresponding bond distances are listed in Table 2.

Deprotonation on the equatorial 4W water molecule results in slight weakening of the Mg−O1B (2.08 Å) and of the Mg−OH_2 (2.10−2.18 Å) bonds, while the formation of a hydroxide ion establishes strong interaction with the metal ion (1.97 Å) as well as a hydrogen bond with O2W (1.76 Å). (It is worth mentioning that a complex hydrogen-bonding network is present in $MgGluc^{+}$ and $MgGlucOH^{0}$, respectively. Such intramolecular interactions were found in the NaGluc and $CaGluc_2^{0}$ solid complexes as well.[74,75]) More importantly, strong hydrogen bonding is seen between O1A and O1W as well as O3 and O3W, as for $MgGluc^{+}$.

Concerning the hydrogen bonding in these species, this unique feature at the molecular level can be related to our macroscopic findings. That is, elongation of the water O−H

DOI: 10.1021/acs.inorgchem.9b00289
Inorg. Chem. 2019, 58, 6832−6844

Table 2. Selected Bond Lengths and Hydrogen Bond Distances (in Å) in the Optimized Structures of the $Mg(H_2O)_5Gluc^+$ and $MgGluc(H_2O)_4(OH)^0$ Complexes[a]

		d(Mg−O)	D[b]	H	A[b]	d(D−H)	d(H···A)
				$MgGluc^+$			
Mg	O1B	2.044	O1W	H(O1W)	O1A	0.995	1.687
Mg	O1W	2.069	O3W	H(O3W)	O3	0.986	1.746
Mg	O2W	2.094	O3	H(O3)	O4	0.969	2.172
Mg	O3W	2.083	O2	H(O2)	O1A	0.974	1.951
Mg	O4W	2.071	O4	H(O4)	O2	0.972	1.920
Mg	O5W	2.093	O6	H(O6)	O4	0.968	1.961
				$MgGlucOH^0$			
Mg	O1B	2.081	O1W	H(O1W)	O1A	0.994	1.694
Mg	OH	1.967	O3W	H(O3W)	O3	0.982	1.765
Mg	O1W	2.115	O3	H(O3)	O4	0.969	2.192
Mg	O2W	2.180	O2	H(O2)	O1A	0.974	1.939
Mg	O3W	2.095	O4	H(O4)	O2	0.973	1.902
Mg	O5W	2.130	O6	H(O6)	O4	0.968	1.956
			O2W	H(O2W)	O(OH)	0.991	1.758

[a]The calculations were performed at the M11/aug-cc-pVTZ level of theory, while solvation effects were considered by applying the CPCM. [b]D: donor oxygen atom. A: acceptor oxygen atom.

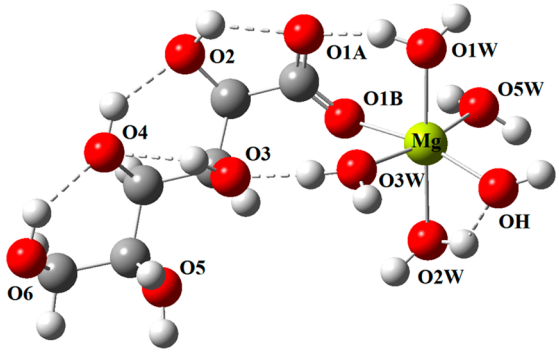

Figure 11. Optimized structure of the $Mg(H_2O)_4(OH)Gluc^0$ complex at the M11 level, applying the aug-cc-pVTZ basis set. The solvation effects were taken into account by utilizing the CPCM. Dashed lines indicate the hydrogen-bonding system.

bonds results in the increased acidity of these H_2O molecules compared to those in the $Mg(H_2O)_6^{2+}$ ion. Hence, coordination of $Gluc^-$ leads to the "ligand-promoted" hydrolysis of Mg^{2+}, and the order of $pK_1 < pK_2 < pK_h$ can be elucidated qualitatively. Additionally, such hydrogen bonds in metal complexes are difficult to discern by conventional NMR measurements.

Furthermore, the formation of both $MgGluc(OH)^0$ and $MgGluc(OH)_2^-$ is facilitated by these hydrogen bonds by lowering the pK value of the ligand. Consequently, $Gluc^-$ is able to keep Mg^{2+} ions in solution without precipitation. To prove this effect, two samples were prepared with $[Mg^{2+}]_T$ = 0.08 M, $[OH^-]_T$ = 0.006 M, and $[L^-]_T$ = 0.17 M, where L^- is gluconate or acetate (Ac^-). For comparison, Ac^- was chosen because it has no OH groups, and the stability of $MgAc^+$ [18,50] is similar to that of $MgGluc^+$. For $Gluc^-$, the formation of $Mg(OH)_2(s)$ was not observed. Conversely, the precipitate was detected right after the addition of NaOH in the case of Ac^-. Because hydrogen bonding between COO^- and H_2O is also possible in the $MgAc^+$ species, the different behavior of $Gluc^-$ highlights the importance of ligand OH groups in the stabilization of Mg^{2+}.

CONCLUSIONS

The complex formation between Mg^{2+} and $Gluc^-$ was studied in neutral-to-alkaline aqueous solutions at 25 °C and 4 M ionic strength. The formation of the $MgGluc^+$ complex was observed and quantitatively described via ^1H and ^{13}C NMR spectroscopic measurements. It was proven by additional IR measurements and quantum-chemical computations that the preferred coordination mode is a pseudobridged monodentate, where one oxygen atom of COO^- is bound to the metal ion, while the other is in hydrogen-bonding interaction with an adjacent OH group.

Further potentiometric titrations revealed the formation of stable, deprotonated complexes, namely, the $MgGlucOH^0$, $MgGluc(OH)_2^-$, and $Mg_3Gluc_2(OH)_4^0$ species; the calcium(II) analogue of the latter was reported earlier. Furthermore, the presence of such a trinuclear complex may be indirect proof for the existence of multinuclear hydroxido complexes of magnesium(II) proposed in the literature.

Because concentrated $MgCl_2$ salt brines might contact with underground radioactive waste disposals, the effect of Mg^{2+} ions on the solubility of actinides is a key factor in the long-term stability assessment of these repositories. Using the stability products obtained in the present work, we calculated the solubility curve of thorium(IV) as a function of pH_c by varying the concentrations of $Gluc^-$ and $MgCl_2$. It was found that, with an increase in the concentration of $MgCl_2$, the solubility of thorium(IV) decreases, which stems from binary complexes forming between the Mg^{2+} and $Gluc^-$ ions. These processes can effectively suppress complexation between $Th(OH)_4(s)$ and $Gluc^-$ at low ligand concentrations.

Additional pH-dependent ^1H and ^{13}C NMR experiments showed that deprotonation does not significantly affect the spectrum of $Gluc^-$. Comparing these spectra with those of the $Ca^{2+}/Gluc^-$ system revealed that, for the magnesium(II) complexes, deprotonation takes place on the coordinated water molecules rather than on the OH groups of the ligand. The main reason for the difference between the two metal complexes is that, in contrast to Ca^{2+}, the OH groups are not directly attached to Mg^{2+}.

On the basis of the titration data, hydrolysis of Mg^{2+} is facilitated by the coordination of $Gluc^-$; this phenomenon can

DOI: 10.1021/acs.inorgchem.9b00289
Inorg. Chem. 2019, 58, 6832−6844

be interpreted on the basis of molecular structures of the $MgGluc^+$ and $MgGlucOH^0$ complexes. DFT calculations showed that, in parallel to ligand binding, two strong hydrogen bonds are established between the COO^- and C3−OH groups of $Gluc^-$ and two metal-bound water molecules, leading to increased acidity of these O−H bonds. Macroscopically, this yields lower p*K* values for the complexes compared to the aqua ion.

In conclusion, ligand-promoted metal-ion hydrolysis appears to be the result of strong hydrogen bonding between the ligand and hydrating water molecules, while the direct binding of ligand OH groups gives rise to metal-ion-induced ligand deprotonation.

■ ASSOCIATED CONTENT

Supporting Information

The Supporting Information is available free of charge on the ACS Publications website at DOI: 10.1021/acs.inorgchem.9b00289.

Detailed description about conversion of the stability/solubility products of the $Th_pGluc_q(OH)_r^{(4p-q-r)+}$ species applying the SIT model, tables listing the converted equilibrium constants and ion interaction parameters, graphical representation of the electrode calibration curves and fitted titration data, optimized structures for the $MgGluc^+$ complex with varying coordination modes, additional speciation diagrams for the $Mg^{2+}/Gluc^-$ and $Ca^{2+}/Gluc^-$ systems, additional solubility curves of thorium(IV), pH-dependent ^{13}C NMR, and temperature-dependent ^1H and ^{13}C NMR spectra (PDF)

■ AUTHOR INFORMATION

Corresponding Author

*E-mail: kutusb@mpip-mainz.mpg.de.

ORCID

Bence Kutus: 0000-0001-5023-0152

István Pálinkó: 0000-0002-8508-309X

Pál Sipos: 0000-0003-1407-0950

Notes

The authors declare no competing financial interest.

■ ACKNOWLEDGMENTS

The authors are thankful to Dr. Gábor Varga and Ákos Buckó for their help in recording the IR and NMR spectra as well as to Shuai Fu for contributing to the preparation of the graphic content of this Article. Financial support of the New National Excellence Programme (Project UNKP-17-3-IV-SZTE-9) and Grants GINOP-2.3.2-15-2016-00013 and NKFIA K 124265 is highly appreciated.

■ REFERENCES

(1) Glasser, F. P.; Atkins, M. Cements in Radioactive Waste Disposal. *MRS Bull.* **1994**, *19*, 33−38.

(2) Berner, U. R. Evolution of Pore Water Chemistry During Degradation of Cement in a Radioactive Waste Repository Environment. *Waste Manage.* **1992**, *12*, 201−219.

(3) Bube, C.; Metz, V.; Bohnert, E.; Garbev, K.; Schild, D.; Kienzler, B. Long-Term Cement Corrosion in Chloride-Rich Solutions Relevant to Radioactive Waste Disposal in Rock Salt − Leaching Experiments and Thermodynamic Simulations. *Phys. Chem. Earth.* **2013**, *64*, 87−94.

(4) Ramachandran, S.; Fontanille, P.; Pandey, A.; Larroche, C. Gluconic Acid: Properties, Applications and Microbial Production. *Food Technol. Biotechnol.* **2006**, *44*, 185−195.

(5) Felmy, A. R. Chemical Speciation of Americium, Curium and Selected Tetravalent Actinides in High Level Waste. *Pacific Northwest National Laboratory Report EMSP-73749*; Pacific Northwest National Laboratory: Richland, WA, 2012.

(6) Colàs, E.; Grivé, M.; Rojo, I.; Duro, L. Solubility of $ThO_2 \bullet xH_2O$(am) in the Presence of Gluconate. *Radiochim. Acta* **2011**, *99*, 269−273.

(7) Warwick, P.; Evans, N.; Hall, T.; Vines, S. Stability Constants of Uranium(IV)-α-IsosaccharinicAcid and Gluconic Acid Complexes. *Radiochim. Acta* **2004**, *92*, 897−902.

(8) Sawyer, D. T.; Kula, R. J. Uranium(VI) Gluconate Complexes. *Inorg. Chem.* **1962**, *1*, 303−309.

(9) Colàs, E.; Grivé, M.; Rojo, I. Complexation of Uranium(VI) by Gluconate in Alkaline Solutions. *J. Solution Chem.* **2013**, *42*, 1545−1557.

(10) Rojo, H.; Tits, J.; Gaona, X.; Garcia-Gutiérrez, M.; Missana, T.; Wieland, E. Thermodynamics of Np(IV) Complexes with Gluconic Acid Under Alkaline Conditions: Sorption Studies. *Radiochim. Acta* **2013**, *101*, 133−138.

(11) Cross, J. E.; Ewart, F. T.; Greenfield, B. F. Modelling the Behaviour of Organic Degradation Products. *MRS Online Proc. Libr.* **1988**, *127*, 715−722.

(12) Moreton, A. D. Thermodynamic Modeling of the Effect of Hydroxycarboxylic Acids on the Solubility of Plutonium at High pH. *MRS Online Proc. Libr.* **1992**, *294*, 753−758.

(13) Tits, J.; Wieland, E.; Bradbury, M. H. The Effect of Isosaccharinic Acid and Gluconic Acid on the Retention of Eu(III), Am(III) and Th(IV) by Calcite. *Appl. Geochem.* **2005**, *20*, 2082−2096.

(14) Coccioli, F.; Vicedomini, M. On the Dissociation of Gluconate Ions and Their Complex Formation with Lead(II) in Alkaline Solution. *J. Inorg. Nucl. Chem.* **1978**, *40*, 2106−2110.

(15) Pallagi, A.; Bajnóczi, É. G.; Canton, S. E.; Bolin, T.; Peintler, G.; Kutus, B.; Kele, Z.; Pálinkó, I.; Sipos, P. Multinuclear Complex Formation between Ca(II) and Gluconate Ions in Hyperalkaline Solutions. *Environ. Sci. Technol.* **2014**, *48*, 6604−6611.

(16) Buckó, Á.; Kutus, B.; Peintler, G.; Pálinkó, I.; Sipos, P. Temperature Dependence of the Acid-Base and Ca^{2+}-Complexation Equilibria of D-gluconate in HyperalkalineAqueous Solutions. *Polyhedron* **2019**, *158*, 117−124.

(17) Gaona, X.; Montoya, V.; Colàs, E.; Grivé, M.; Duro, L. Review of the Complexation of Tetravalent Actinides by ISA and Gluconate UnderAlkaline to HyperalkalineConditions. *J. Contam. Hydrol.* **2008**, *102*, 217−227.

(18) Cannan, R. K.; Kibrick, A. Complex Formation Between Carboxylic Acids and Divalent Metal Cations. *J. Am. Chem. Soc.* **1938**, *60*, 2314−2320.

(19) Carper, W. R.; Coffin, D. B.; Addis, J. R. Studies of Magnesium and Manganese Interactions with Gluconate and 1,5-Gluconolactone. *Spectrochim. Acta* **1989**, *45A*, 391−392.

(20) Bailey, G. D.; Carper, W. R. ^{13}C Relaxation Studies of Gluconate and Magnesium-Gluconate Interactions. *J. Inorg. Biochem.* **1993**, *52*, 99−108.

(21) Coffin, D. B.; Carper, W. R. Carbon-13 NMR Relaxation Studies of Gluconate and Manganese-Gluconate Interactions. *Magn. Reson. Chem.* **1988**, *26*, 591−594.

(22) Carper, W. R.; Coffin, D. B. NMR Studies of Paramagnetic Metal Ion Interactions with Gluconate and 1,5-Gluconolactone. *Inorg. Chim. Acta* **1990**, *167*, 261−264.

(23) Horton, D.; Wałaszek, Z.; Ekiel, I. Conformations of D-Gluconic, D-Mannonic, and D-Galactonic Acids in Solution, as Determined by N.M.R. Spectroscopy. *Carbohydr. Res.* **1983**, *119*, 263−268.

(24) Sipos, P.; May, P. M.; Hefter, G. T. Carbonate Removal from Concentrated Hydroxide Solutions. *Analyst* **2000**, *125*, 955−958.

DOI: 10.1021/acs.inorgchem.9b00289
Inorg. Chem. 2019, 58, 6832−6844

(25) Peintler, G.; Kormányos, B.; Gyurcsik, B. *pHCali*, version 1.32a-20070323; University of Szeged, Szeged, Hungary, 2007.
(26) Crea, F.; Stefano, C.; Gianguzza, A.; Piazzese, D.; Sammartano, S. Protonation of Carbonate in Aqueous Tetraalkylammonium Salts at 25°C. *Talanta* **2006**, *68*, 1102−1112.
(27) Zékány, L.; Nagypál, I.; Peintler, G. *PSEQUAD for Chemical Equilibria*, update 5-5.10; Sprinker: Budapest, Hungary, 2000−2008.
(28) Puigdomenech, I. *MEDUSA*, version 1; KTH Royal Institute of Technology: Stockholm, Sweden, 2015.
(29) Rand, M.; Fuger, J.; Grenthe, I.; Neck, V.; Rai, D. Chemical Thermodynamics of Thorium. In *Chemical Thermodynamics.*; Mompean, F. J., Perrone, J., Illemassène, M., Eds.; OECD Publications: Paris, France, 2011; Vol. *11*.
(30) Neck, V.; Kim, J. I. Solubility and Hydrolysis of Tetravalent Actinides. *Radiochim. Acta* **2001**, *89*, 1−16.
(31) Brønsted, J. N. Studies of Solubility: IV. The Principle of Specific Interaction of Ions. *J. Am. Chem. Soc.* **1922**, *44*, 877−898.
(32) Brønsted, J. N. Calculation of the Osmotic and Activity Functions in Solutions of Uni-Univalent salts. *J. Am. Chem. Soc.* **1922**, *44*, 938−948.
(33) Scatchard, G. Concentrated Solutions of Strong Electrolytes. *Chem. Rev.* **1936**, *19*, 309−327.
(34) Guggenheim, E. A. *Applications of Statistical Mechanics*; Clarendon Press: Oxford, U.K., 1966.
(35) Pitzer, K. S. *Activity Coefficients in Electrolyte Solutions*, 2nd ed.; CRC Press: Boca Raton, FL, 1991.
(36) Bretti, C.; Foti, C.; Sammartano, S. Calculation of SIT Parameters. Part I. A New Approach in the Use of SIT in Determining the Dependence on Ionic Strength of Activity Coefficients. Application to Some Chloride Salts of Interest in the Speciation of Natural Fluids. *Chem. Speciation Bioavailability* **2004**, *16*, 105−110.
(37) Jiménez-Reyes, M.; Solache-Ríos, M.; Rojas-Hernández, A. Application of the Specific Ion Interaction Theory to the Solubility Product and First Hydrolysis Constant of Europium. *J. Solution Chem.* **2006**, *35*, 201−214.
(38) Sipos, P. Application of the Specific Ion Interaction Theory (SIT) for the Ionic Products of Aqueous Electrolyte Solutions of Very High Concentrations. *J. Mol. Liq.* **2008**, *143*, 13−16.
(39) Fellhauer, D.; Altmaier, M.; Gaona, X.; Lützenkirchen, J.; Fanghänel, T. Np(V) Solubility, Speciation and Solid Phase Formation in Alkaline $CaCl_2$ Solutions. Part II: Thermodynamics and Implications for Source Term Estimations of Nuclear Waste Disposal. *Radiochim. Acta* **2016**, *104*, 381−397.
(40) Yalçıntaş, E.; Gaona, X.; Altmaier, M.; Dardenne, K.; Polly, R.; Geckeis, H. Thermodynamic Description of Tc(IV) Solubility and Hydrolysis in Dilute to Concentrated NaCl, $MgCl_2$ and $CaCl_2$ Solutions. *Dalton. Trans.* **2016**, *45*, 8916−8936.
(41) Altmaier, M.; Yalçıntaş, E.; Gaona, X.; Neck, V.; Müller, R.; Schlieker, M.; Fanghänel, T. Solubility of U(VI) in Chloride Solutions. I. The Stable Oxides/Hydroxides in NaCl Systems, Solubility Products, Hydrolysis Constants and SIT Coefficients. *J. Chem. Thermodyn.* **2017**, *114*, 2−13.
(42) Ciavatta, L. The Specific Interaction Theory in Evaluating Ionic Equilibria. *Ann. Chim. (Rome).* **1980**, *70*, 551−567.
(43) Peverati, R.; Truhlar, D. G. Improving the Accuracy of Hybrid Meta-GGA Density Functionals by Range Separation. *J. Phys. Chem. Lett.* **2011**, *2*, 2810−2817.
(44) Cossi, M.; Rega, N.; Scalmani, G.; Barone, V. Energies, Structures and Electronic Properties of Molecules in Solution with the C-PCM Solvation Model. *J. Comput. Chem.* **2003**, *24*, 669−681.
(45) *Gaussian09*, revision E.01; Gaussian, Inc.: Wallingford, CT, 2013.
(46) Pallagi, A.; Sebók, P.; Forgó, P.; Jakusch, T.; Pálinkó, I.; Sipos, P. Multinuclear NMR and Molecular Modelling Investigations on the Structure and Equilibria of Complexes That Form in Aqueous Solutions of Ca^{2+} and Gluconate. *Carbohydr. Res.* **2010**, *345*, 1856−1864.
(47) Lewis, D.; Lund, A.; Vänngård, T.; Håkansson, R.; Munch-Petersen, J. Studies on the Hydrolysis of Metal Ions. The Hydrolysis of Magnesium in Chloride Self-Medium. *Acta Chem. Scand.* **1963**, *17*, 1891−1901.
(48) Kutus, B.; Gácsi, A.; Pallagi, A.; Pálinkó, I.; Peintler, G.; Sipos, P. A Comprehensive Study on the Dominant Formation of the Dissolved $Ca(OH)_2(aq)$ in Strongly Alkaline Solutions Saturated by Ca(II). *RSC Adv.* **2016**, *6*, 45231−45240.
(49) Xiong, Y. Thermodynamic Properties of Brucite Determined by Solubility Studies and Their Significance to Nuclear Waste Isolation. *Aquat. Geochem.* **2008**, *14*, 223−238.
(50) Martell, A.; Smith, R. M. Other Organic Ligands. In *Critical Stability Constants*; Martell, A.. Ed.; Springer: New York, 1977; Vol. *3*.
(51) Portanova, R.; Lajunen, L. H. J.; Tolazzi, M.; Piispanen, J. Critical Evaluation of Stability Constants for α-Hydroxycarboxylic Acid Complexes with Protons and Metal Ions and the Accompanying Enthalpy Changes. Part II. Aliphatic 2-Hydroxycarboxylic Acids. IUPAC Techical Report. *Pure Appl. Chem.* **2003**, *75*, 495−540.
(52) Smirnov, P. R.; Trostin, V. N. Structural Parameters of Hydration of Be^{2+} and Mg^{2+} Ions in Aqueous Solutions of Their Salts. *Russ. J. Gen. Chem.* **2008**, *78*, 1643−1649.
(53) Di Tommaso, D.; De Leeuw, N. H. Structure and Dynamics of the Hydrated Magnesium Ion and of the Solvated Magnesium Carbonates: Insights from First Principles Simulations. *Phys. Chem. Chem. Phys.* **2010**, *12*, 894−901.
(54) Bai, G.; Yi, H.-B.; Li, H.-J.; Xu, J.-J. Hydration Characteristics of Ca^{2+} and Mg^{2+}: A Density Functional Theory, Polarized Continuum Model and Molecular Dynamics Investigation. *Mol. Phys.* **2013**, *111*, 553−568.
(55) Van Panthaleon van Eck, C. L.; Mendel, H.; Boog, W. X-Ray Diffraction of Aqueous Electrolyte Solutions. *Discuss. Faraday Soc.* **1957**, *24*, 200−205.
(56) Probst, M. M.; Radnai, T.; Heinzinger, K.; Bopp, P.; Rode, B. M. Molecular Dynamics and X-Ray Investigation of an Aqueous Calcium Chloride Solution. *J. Phys. Chem.* **1985**, *89*, 753−759.
(57) Fulton, J. L.; Heald, M. S.; Badyal, Y. S.; Simonson, J. M. Understanding the Effects of Concentration on the Solvation Structure of Ca^{2+} in Aqueous Solution. I: The Perspective on Local Structure from EXAFS and XANES. *J. Phys. Chem. A* **2003**, *107*, 4688−4696.
(58) Megyes, T.; Grosz, T.; Radnai, T.; Bako, I.; Palinkas, G. Solvation of Calcium Ion in Polar Solvents: An X-ray Diffraction and Ab Initio Study. *J. Phys. Chem. A* **2004**, *108*, 7261−7271.
(59) Rudolph, W. W.; Irmer, G. Hydration of the Calcium(II) Ion in an Aqueous Solution of Common Anions (ClO_4^-, Cl^-, Br^-, and NO_3^-). *Dalton Trans.* **2013**, *42*, 3919−3935.
(60) Rodriguez-Cruz, S. E.; Jockusch, R. A.; Williams, E. R. Hydration Energies and Structures of Alkaline Earth Metal Ions, $M^{2+}(H_2O)_n$, n = 5−7, M = Mg, Ca, Sr, and Ba. *J. Am. Chem. Soc.* **1999**, *121*, 8898−8906.
(61) Nickolov, Zh.; Georgiev, G.; Stoilova, D.; Ivanov, I. Raman and IR Study of Cobalt Acetate Dihydrate. *J. Mol. Struct.* **1995**, *354*, 119−125.
(62) Binitha, M. P. Studies on Growth and Properties of Some Metal Succinate Crystals. Ph.D. Thesis, University of Calicut, Calicut, India, 2014; p 61.
(63) Tajmir-Riahi, H. A. Carbohydrate Complexes with Alkaline Earth Metal Ions. Interaction of D-Glucono-1,5-Lactone with the Mg(II), Ca(II), Sr(II), and Ba(II) Cations in the Crystalline Solid and Aqueous Solution. *J. Inorg. Biochem.* **1990**, *39*, 33−41.
(64) Deacon, G. B.; Phillips, R. J. Relationships Between the Carbon-Oxygen Stretching Frequencies of Carboxylato Complexes and the Type of Carboxylate Coordination. *Coord. Chem. Rev.* **1980**, *33*, 227−250.
(65) Papageorgiou, S. K.; Kouvelos, E. P.; Favvas, E. P.; Sapalidis, A. A.; Romanos, G. E.; Katsaros, F. K. Metal−Carboxylate Interactions in Metal−Alginate Complexes Studied with FTIR Spectroscopy. *Carbohydr. Res.* **2010**, *345*, 469−473.
(66) Einaga, H. Hydrolysis of Magnesium(II) in 1.0 $moldm^{-3}$ Aqueous $(Na,H)NO_3$ Solution. *J. Chem. Soc., Dalton Trans.* **1977**, 912−914.

DOI: 10.1021/acs.inorgchem.9b00289
Inorg. Chem. 2019, 58, 6832−6844

(67) Burkov, K. A.; Bus'ko, E. A.; Garmash, L. A.; Khonin, G. V. Hydrolysis of Magnesium Perchlorate at 25−140 °C. *Zh. Neorg. Khim.* **1978**, *23*, 1767−1772.
(68) Ekberg, C.; Brown, P. L. *Hydrolysis of Metal Ions.*; Wiley-VCH, Weinheim, Germany, 2016.
(69) Van Duin, M.; Peters, J. A.; Kieboom, A. P. G.; Van Bekkum, H. A General Coordination-Ionization Scheme for Polyhydroxy Carboxylic Acids in Water. *Recl. Trav. Chim. Pays-Bas.* **1989**, *108*, 57−60.
(70) Motekaitis, R. J.; Martell, A. E. Complexes of Aluminum(II1) with Hydroxy Carboxylic Acids. *Inorg. Chem.* **1984**, *23*, 18−23.
(71) Lakatos, A.; Kiss, T.; Bertani, R.; Venzo, A.; Di Marco, V. B. Complexes of Al(III) with D-Gluconic Acid. *Polyhedron* **2008**, *27*, 118−124.
(72) Giroux, S.; Rubini, P.; Henry, B.; Aury, S. Complexes of Praseodymium(III) with D-Gluconic Acid. *Polyhedron* **2000**, *19*, 1567−1574.
(73) Jeffrey, J. A. *An Introduction to Hydrogen Bonding.*; Oxford University Press: New York, 1997.
(74) Di, Y.-Y.; Zhang, Y.-H.; Liu, Y.-P.; Kong, Y.-X.; Zhou, C.-S. Crystal Structure and Thermodynamic Properties of Sodium D-Gluconate Na[D-$C_6H_{11}O_7$](s). *J. Therm. Anal. Calorim.* **2017**, *127*, 1835−1843.
(75) Bugris, V.; Dudás, Cs.; Kutus, B.; Harmat, V.; Csankó, K.; Brockhauser, S.; Pálinkó, I.; Turner, P.; Sipos, P. Crystal and Solution Structures of Calcium Complexes Relevant to Problematic Waste Disposal: Calcium Gluconate and Calcium Isosaccharinate. *Acta Crystallogr., Sect. B: Struct. Sci., Cryst. Eng. Mater.* **2018**, *74*, 598−609.

DOI: 10.1021/acs.inorgchem.9b00289
Inorg. Chem. 2019, 58, 6832−6844